BENCHMARKING FENDL LIBRARIES THROUGH ANALYSIS OF BULK SHIELDING EXPERIMENTS ON LARGE SS316 ASSEMBLIES FOR VERIFICATION OF ITER SHIELDING CHARACTERISTICS

Mahmoud Z. Youssef*, Anil Kumar*, Mohamed A. Abdou*, Chikara Konno**, Fujio Maekawa**, Masayuki Wada**, Yukio Oyama**, Hiroshi Maekawa**, And Yujiro Ikeda**

*School of Engineering and Applied Science,
University of California at Ls Angeles
Los Angeles, CA, 90095, USA
(310) 825-2879

** Department of Reactor Engineering,
Japan Atomic Energy Research Institute,
Tokai-mura, Ibaraki-ken 319-11, Japan
81-292-82-6074

ABSTRACT

FENDL-1 data base has been developed recently for use in ITER/EDA phase and other fusion-related design activities. It is now undergoing extensive testing and benchmarking using experimental data of differential and integral measured parameters obtained from fusion-oriented experiments. As part of co-operation between UCLA (U.S.) with JAERI (Japan) on executing the required neutronics R&D tasks for ITER shield design, two bulk shielding experiments on large SS316 assemblies were selected for benchmarking FENDL/MG-1 multigroup data base and FENDL/MC-1 continous energy data base. The analyses with the multigroup data (performed with S8, P5, DORT calculations with shielded and unshielded data) also included library derived from ENDF/B-VI data base for comparison purposes. The MCNP Monte Carlo code was used by JAERI with the FENDL/MC-1 data. The results of this benchmarking is reported in this paper along with the observed deficiencies and discrepancies.

I. INTRODUCTION

The Nuclear data Section (NDS) of the International Atomic Energy Agency (IAEA) has provided the fusion community with the first version of an internationally available Fusion Nuclear Data Library[1], FENDL-1 that was achieved as a result of cooperation between several national nuclear data centers around the world. This library is intended to be used in the Engineering Design Phase (EDA) of the International Thermonuclear Experimental Reactor, ITER[2-4]. The major two files of the many FENDL-1 files[1] are FENDL/MG-1.0 and FENDL/MC-1.0 files (multi-group, MG, and continous energy Monte Carlo, MC) and they are undergoing an extensive benchmarking[5-6] in order to provide high quality assurance data base for ITER designers

Two integral experiments were selected in the present study, which are relevant to ITER inboard/outboard shield design. They are those conducted at the Fusion Neutronics Source (FNS) facility at JAERI, namely: (1) Bulk shielding experiment on a 1.2 m ϕ by 1.1176 L m cylindrical assembly of SS316 without a source can (Assembly#1), and (2) Bulk shielding experiment on a 1.2 m by 1. 1176 m cylindrical assembly of SS316 with a source can (source reflector of 0.2 m thickness). (Assembly#2).

The purpose of the reported analysis is twofold: (a) identifying deficiencies, if any, in FENDL/MG-1 and MC data by comparing analytical results to measured items that have high precision (small experimental errors) and (b) verifying the adequacy of the library in predicting neutronics parameters at deep locations inside a thick shield and quantifying ranges of uncertainties (design margins) of calculated parameters that impact magnet protection scheme in ITER[7-8]. As a reference, the analysis was also performed with ENDF/B-VI data. In addition, it was necessary to generate data libraries that include self-shielding correction for SS316 cross-sections. The results based on shielded and unshielded cross-section libraries are compared in the present work. More details of the present work can be found in Ref. 9. The experimental data of the first two assemblies have been published recently[10] along with analysis based on JENDL-3.1 data[11] .

Section II describes the experiments and the measured items. Description of the procedures followed in the analysis is given in Section III. Results of FENDL-1 and ENDF/B-VI benchmarking are given in Section IV. Section V is devoted to the observed discrepancies between the analytical results and measured data and their impact on ITER shield design.

II. DESCRIPTION OF THE EXPERIMENTS

Figure 1 shows the geometrical arrangement of the two bulk shielding experiments listed above. The function of the source can is to give arise to a more prototypical condition of the incident neutron found in ITER device (including a reflected neutron component), on one hand, and to reduce the effect of the neutron room-return component,

on the other[12]. The atomic densities of the materials present in each zone are given in Table 1.

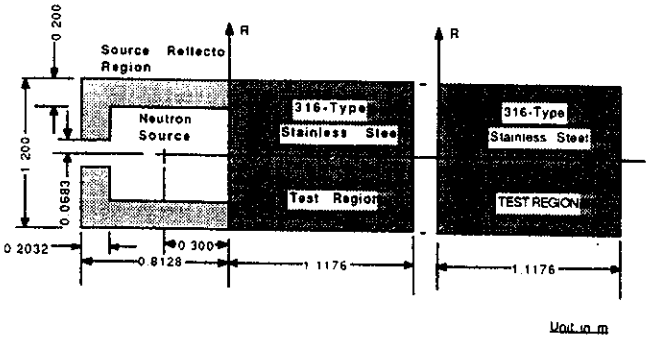

Figure 1 : The Geometry of the two Assemblies considered

Neutron spectrum, foil activation reaction rates of various threshold energies, fission reaction rates and gamma-ray heating were measured at several location along the axis of the assembly up to a depth of 914 cm. The activation reactions considered are $^{27}Al(n,\alpha)^{24}Na$, $Ti(n,x)^{46}Sc$, $Ti(n,x)^{47}Sc$, $Ti(n,x)^{48}Sc$, $Fe(n,x)^{56}Mn$, $^{59}Co(n,a)^{56}Mn$, $^{58}Ni(n,2n)^{57}Ni$, $^{58}Ni(n,p)^{58}Co$, $^{64}Zn(n,p)^{64}Cu$, $^{90}Zr(n,2n)^{89}Zr$, $^{93}Nb(n,2n)^{92m}Nb$, $^{115}In(n,n')^{115m}In$, $^{197}Au(n,g)^{198}Au$. The fission rates measured were $^{35}U(n,f)$, $^{238}U(n,f)$. The location of measurements are: 0.0, 127.0, 228.6, 330.2, 457.2, 609.6, 711.2, 914.4 cm from the front surface of the assembly. Neutron spectrum was also measured at z=-10mm. The largest depth (0.914 m) is much larger than those found in previous bulk shielding experiments. With the verification of attenuation characteristics of SS316 assemblies at deep locations, and with the ability to measure the neutron flux at various energy rages (e.g. >10 MeV, 2-10 MeV, 0.1-1 MeV, 10-100 keV, 1-10 keV, 0.1-1 keV, 10-100 eV and 1-10 eV), the observed discrepancies between calculations and measurements are more representative to those anticipated in ITER inboard/outboard shield over a wide range of neutron energies. The Calculated-to-the Experimental (C/E) values for the integrated neutron spectrum in the above mentioned energy ranges are given in the present work in addition to the C/E values for the other items listed above.

III. CALCULATION PROCEDURES

A. Cross-Section Data Libraries

The 175n-42g FENDL/MG-1.0 in MATXS format[13] (denoted MATXS15) was used in the benchmarking. The counterpart library based on ENDF/B-VI (175n-42g) is denoted by MATXS14 Four data libraries were generated in group-independent (GIP) form using the TRANSX2 processing code package[13], namely shielded and unshielded MG libraries based on FENDL/MG-1 and shielded and unshielded libraries based on ENDF/B-VI. Self-shielding was considered an important correction to the multigroup constants. The total macroscopic cross-section of SS316 has many resonances in the energy range keV to few MeV. Neutrons lose energies through either elastic (many collisions) or inelastic collisions and ignoring the presence of these resonances will give an inaccurate flux estimates in SS316, particularly at deep locations and for low-energy neutrons. It was shown that the unshielded SS316 total macroscopic cross-section (infinite dilution case) is a factor of 1.2-2 higher than the shielded one at several resonances leading to lower neutron flux at deep locations. At present, the current dosimetry reactions in MATXS15 are based on ENDF/B-VI[14]. For reactions that are currently not available in MATXS15 [e.g. $^{235}U(n,f)$, $^{238}U(n,f)$, $^{115}In(n,n')^{115m}In$, $^{64}Zn(n,p)^{64}Cu$] or MATXS14 [e.g. previous reactions plus $^{93}Nb(n,2n)^{92m}Nb$], the dosimetry file of JENDL-3.1 (J3DF) of the 125n multigroup form was used instead[15]. The fine-group libraries mentioned above were condensed to 80n-24g libraries (along with the dosimetry cross-sections) and used in the subsequent transport calculations. The ANISN code[16] was used to generate these weighted fewer-multigroup libraries according to a 1-D slab model that simulated Assembly #2.

Table 1 : Atomic Densities of Materials Used in the Analysis

Nuclide**	SS316 (Test Region)	SS316 (Reflector Region)	Air	Water
H-1 (E/B6.1)				6.6659e-2
N-14 (B2)			3.8810e-5	
O-16 (E/B6.0)			1.0400e-5	3.3329e-2
Si (B2)	1.0341e-3*	8.1608e-4	-	-
Cr (E/B6.1)	1.5482e-2	1.5025e-2	-	-
Mn-55 (E/B6.0-J3)	1.0355e-3	1.3561e-3	-	-
Fe (E/B6.1)	5.7904e-2	5.8331e-2	-	-
Ni (E/B6.1)+	9.3405e-3	9.1456e-3	-	-
Mo (J3.1)	1.0585e-3	1.0254e-3	-	-

* Reads: 1.0341 X 10^{-3} Atoms/cm^3 X 10^{-24}
** E/B6.1 (ENDF/B-VI.1)- B2: BROND-2- J3.1: JENDL-3.1
+ Except Ni-61 (from E/B6.0)

As for the Monte Carlo calculations, the FENDL/MC-1.0 continous energy library was used. The 125n-40g group structure of the Japanese library FUSION-J3[11] was used for the energy bins of the tallies. No self-shielding correction was needed in this case since continous energy treatment was applied throughout the calculations.

B. The Angular/Energy Distribution of the Incident Neutron Source

The angular/energy distribution of the emitted neutrons from the tritiated-titanium target was calculated by JAERI, using the MORSE-DD code[17], in 125-n group structure and 37 angles spanning (in 5-degree intervals) the directions from μ=-1 (180-degree) to μ=+1 (0-degree) along the z-axis.

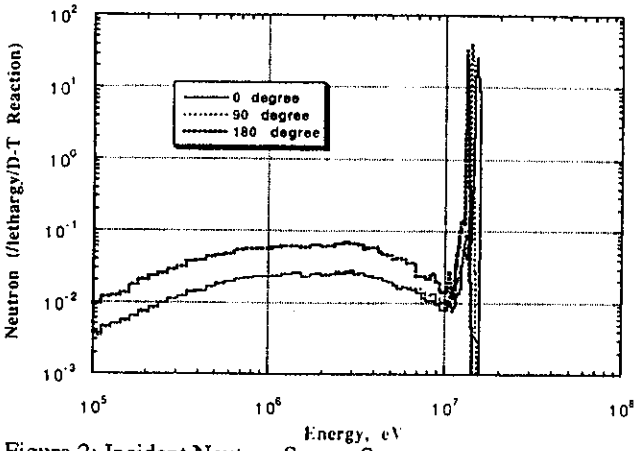

Figure 2: Incident Neutron Source Spectrum

The slowing down of deuteron ions in the TiT target, the shape of the deuteron beam, the kinematics of the D-T reactions, cross-section of the D-T reaction at each deuteron energy, and the accurate description of the structural shape of the TiT target were considered in generating the source. Figure 2 shows the source neutron spectrum at μ=+1 (0-degree), μ=0 (90-degree), and μ=-1 (180-degree). The peak energy in the forward direction is at 14.8 MeV whereas it is 13.3 MeV in the backward direction. Non-negligible low-energy component of the source spectra can be seen in the figure due to the interaction of the D-T neutrons with the structural material of the TiT target.

C. Discrete Ordinates and Monte Carlo Calculations

To eliminate the ray-effect, the RUFF code[18] was used to generate the uncollided flux and the first collision source used as input for the 2-D discrete ordinates code, DORT[19] in R-Z geometry. Because of neutron multiplication in the target structure, the number of neutrons emitted from the target per D-T reaction was found to be ~1.0295. The DORT calculations were performed with P5S8 approximations. A typical mesh size in the reflector (can) and the test region were 0.2-0.4 cm particularly at the front surface and around measuring locations.

In MCNP MC calculations, the dependency of the source neutrons on angle and energy were considered in the source subroutine which includes sampling procedures. Source neutrons were emitted towards the whole solid angle in Assembly#2 and inside a cone of 63.4 degree in Assembly#1. Surface flux estimators were used for the standard detectors. A typical detector size of 40 mm was used at the 9 measuring locations. The number of histories varied between 1-4 millions, depending on the calculated response under consideration.

IV. ANALYTICAL RESULTS AND COMPARISON WITH MEASUREMENTS

A. Neutron Spectrum and Reaction Rates

The calculated neutron spectrum in the MeV energy range with the 80n-24g were smeared using the NE213 energy windows and the results are denoted FENDL (SS-smeared) in the figures. The No smearing cases are denoted NS (SS stands for Self-Shielded libraries).

1. Energy range > 10 MeV: In Assembly #1 , the spectra > 10 MeV is well predicted at front locations but, on the average, the calculated spectrum tends to fall below the experimental values as the depth increases inside the test region as can be seen in Fig. 3 for the integrated

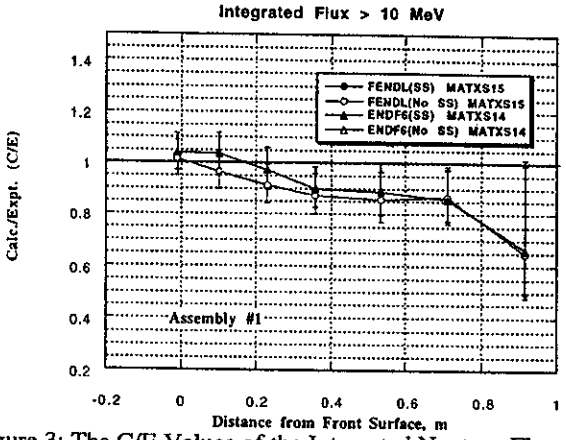

Figure 3: The C/E Values of the Integrated Neutron Flux above 10 MeV- FENDL/MG (Assembly #1)

spectrum in Ass.#1 The calculated spectrum is within 15% of the experimental values (FENDL/MG, ENDF6/MG) at front locations but large under estimation (~35% FENDL/MG, ~10% FENDL/MC, see Fig. 4) occurs at depth 0.914 m where the experimental error is large

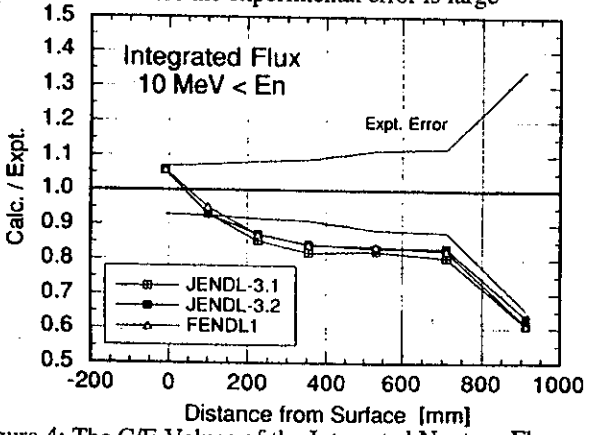

Figure 4: The C/E Values of the Integrated Neutron Flux above 10 MeV- FENDL/MC (Assembly #1)

This has implication on the C/E values of reactions whose thresholds are above 10 MeV such as ^{58}Ni(n,2n)^{57}Ni and

$^{90}Zr(n,2n)^{89}Zr$ where their C/E values are below unity and the underprediction increases by depth as shown in Fig. 5. (The MCNP calculations performed by JAERI show also results based on JENDL-3.1 and 3.2 for comparison. We focus here on FENDL results). As expected, the self-shielding corrections have no impact on high threshold reactions or the high-energy neutron spectrum in the MeV range. The above features are similar in Assembly #2. The

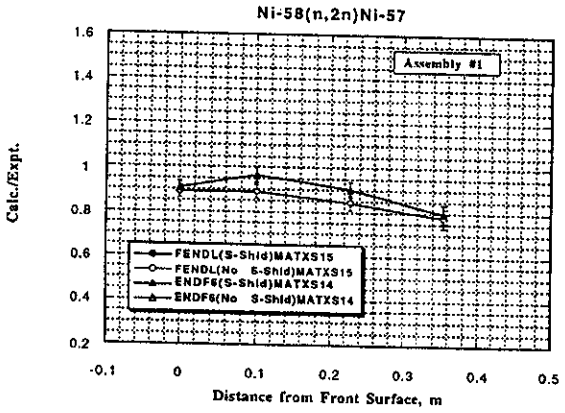

Figure 5: The C/E values for $^{58}Ni(n,2n)^{57}Ni$ (Assemb#1)

$^{93}Nb(n,2n)^{92m}Nb$ reaction has a threshold around 8 MeV and increases by energy then saturates around 14 MeV. The C/E curve for this reaction is also under predicted by FENDL/MG in both assemblies by ~20% at depth 0.533. The C/E values of the $^{238}U(n,f)$ reaction are similar to those of the high-energy threshold reactions. In both assemblies, results based on ENDF6/MG libraries are larger than the ones obtained by FENDL/MG by ~5-7%, particularly at front locations.

2. Energy Range 2-10 MeV: In this energy range, the integrated spectrum based on FENDL/MG calculations is generally over predicted at front locations (by as much as 30-50% at the surface) and the over prediction decreases by depth. Note that the experimental error in this energy range is large (particularly at the front surface, see Figs. 6-7). Beyond ~ 0.44 m in Assembly #1 (0.4 m in Assembly #1), the integrated spectrum is under predicted. At depth 0.533 m, the underprediction by FENDL/MG is ~20% in Assembly #2 (10% in Assembly #1). Reactions that have their threshold in the energy range 5-10 MeV are $^{93}Nb(n,2n)^{92m}Nb$, $^{27}Al(n,\alpha)^{24}Na$, and $^{59}Co(n,a)^{56}Mn$ Nevertheless, these reactions are under predicted by FENDL at nearly all locations due mainly to the under prediction in the integrated spectrum above 10 MeV which contibutes the most to these reactions. Reactions that have their threshold in the energy range 2-5 MeV are $Ti(n,x)^{46}Sc$, $^{64}Zn(n,p)^{64}Cu$, and $^{58}Ni(n,p)^{58}Co$. These reactions show C/E values larger than unity at front locations and lower than unity at locations beyond 0.36 m and thus follow the same trend of the integrated spectrum, as can be seen in Figs. 8-9 for $^{64}Zn(n,p)^{64}Cu$.

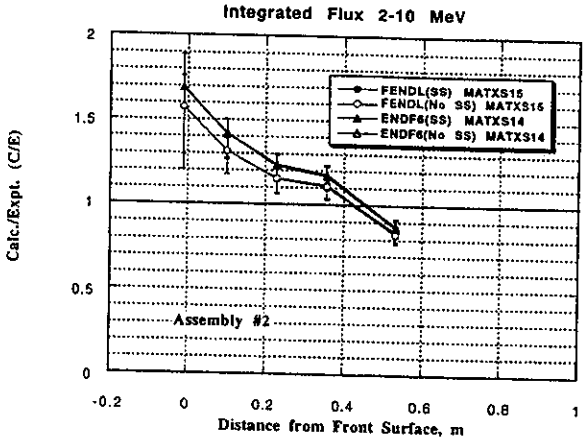

Figure 6: The C/E Values of the Integrated Neutron Flux in the Energy Range 2-10 MeV -FENDL/MG

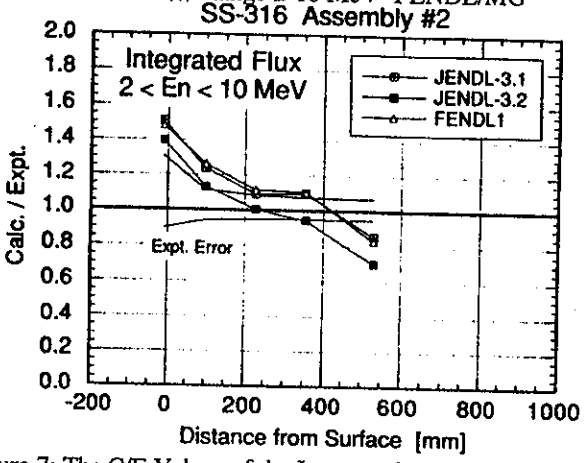

Figure 7: The C/E Values of the Integrated Neutron Flux in the Energy Range 2-10 MeV-FENDL/MC

For example, the C/E values for the $^{64}Zn(n,p)^{64}Cu$ reaction is over predicted at the front and under predicted by ~20% in Assembly #1 and ~30% in Assembly #2 at depth 0.533 m. As is the case in the energy range above 10 MeV, the effect of self-shielding correction is negligible in this energy range. The underorediction with the MC data is within the experimental error (~10%, see Fig. 9).

3. Energy Range 0.1-1 MeV: Generally, the effect of self-shielding the SS316 cross-section is more apparent for energies below 1 MeV where results based on the shielded cross-sections are closer to the experimental values. Except for the first measuring location at -0.01 m, the trend of the C/E values of the integrated spectrum is similar in Assembly #1 and #2, that is, close values to unity at shallower locations followed by under prediction

starts at depth 0.2 m which increases by depth., as can be seen from Figs. 10-11. Based on FENDL/MG data,

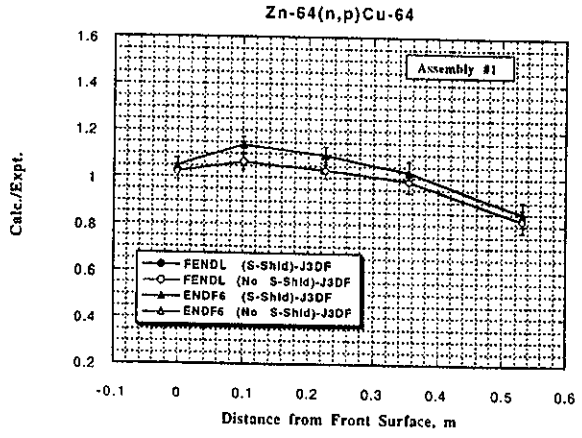

Figure 8: The C/E values for $^{64}Zn(n,p)^{64}Cu$-FENDL/MG (Assembly#1)

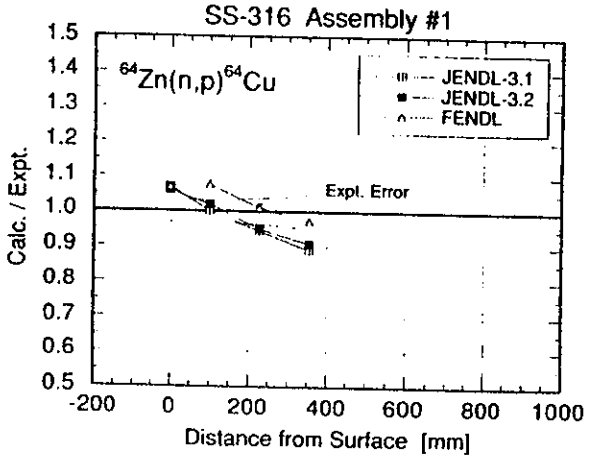

Figure 9: The C/E values for $^{4}Zn(n,p)^{64}Cu$-FENDL/MC (Assembly#1)

the underprediction at depth 0.9144 m is ~60% in both assemblies with the MG data and ~15-25% with the MC data. Results based on ENDF6 data are larger by 5-10%. The influence of the self-shielding correction is more manifested at deeper locations. The integrated spectra calculated with the unshielded FENDL/MG cross-sections are within ~2-5% of the experimental values at front locations (up to ~0.2 m) but they are much lower than measured data at deep locations (by as much as ~ 80% in both assemblies at depth 0.9144). The difference in the results based on FENDL/MG and ENDF6/MG data is less pronounced than the difference between the shielded and unshielded cases. As for the reaction rates, the $^{115}In(n,n')^{115m}In$ reaction has threshold (at ~ 0.5 MeV) that falls within this energy range and more sensitive to neutrons in the energy range 1-10 MeV than to the 14 MeV neutrons. Features of its C/E values are similar to the integrated spectrum in the 0.1-1 MeV range as can be seen in Figs. 12-13.

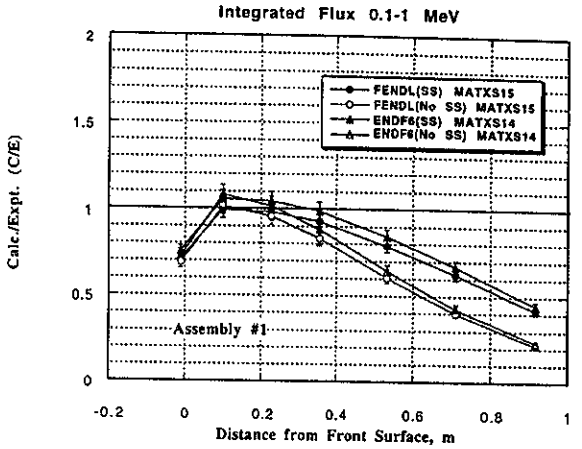

Figure 10: The C/E Values of the Integrated Neutron Flux in the Energy Range 0.1-1 MeV - FENDL/MG

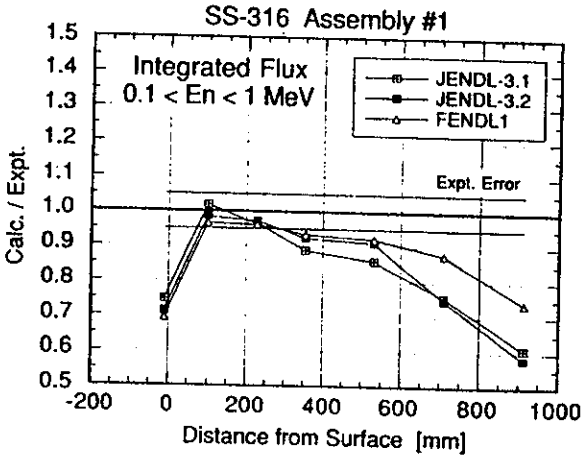

Figure 11: The C/E Values of the Integrated Neutron Flux in the Energy Range 0.1-1 MeV - FENDL/MC

4. Energy range 10-100 keV: Except for the first measuring location at -0.01m, the shape of the C/E curves of the integrated spectrum in this energy range is similar in the two assemblies. Both FENDL/MG and ENDF6/MG data overestimate the integrated spectrum up to a depth 0.45 m (FENDL) and 0.533 m (ENDF6). The maximum over estimation up to this depth obtained by FENDL/MG shielded data is ~ 15% (Assembly #1) and ~ 20 % (Assembly #2). Larger over estimation (20-40%) is obtained with the unshielded data (see discussion below). The under prediction starts to be observed at larger depth. Based on FENDL/MG data, the under prediction at depth

0.9144 m is ~40% in both assemblies (see Fig. 14) Results based on ENDF6 data are larger by 5-10%. The effect of the self-shielding correction is more pronounced at

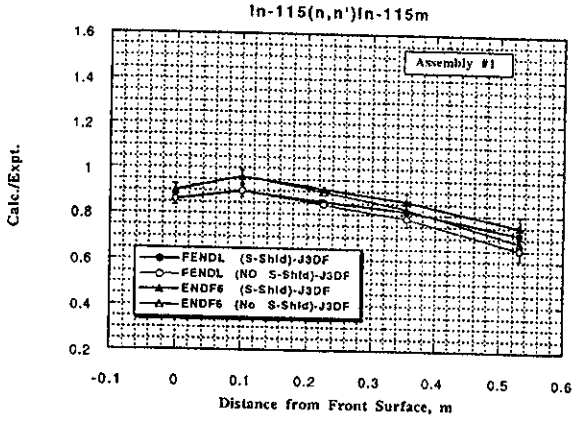

Figure12: The C/E values for $^{115}In(n,n')^{115m}In$ FENDL/MG-(Assembly #1)

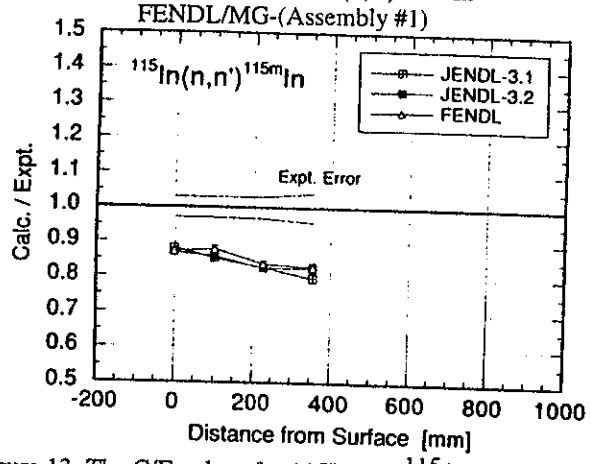

Figure 13: The C/E values for $115In(n,n')^{115m}In$ FENDL/MC-(Assembly #1)

deeper locations than in case of 0.1-1 MeV integrated flux. At depth 0.914 m, the integrated spectra calculated with the unshielded FENDL/MG is underpredicted by as much as 60-70%. Results based on FENDL/MC data are similar to those based on the shielded MG data, as can be seen from Fig. 15. The under prediction at the deepest location is ~20%.

One can notice from the spectrum comparison curves shown in Fig. 16 that the neutron flux in this energy range calculated by the unshielded cross-sections is larger than the one obtained by the shielded cross-sections up to a depth of ~0.3 m in assembly #1 (~0.25 m in Assembly #2). It was shown that the reverse is true for other integrated spectra at higher energies. This can be explained by examining the total macroscopic cross-section of the SS316 shown in Fig. 17. In the case of unshielded cross-sections, the several resonances in the 100 keV range and the much larger resonance at 30 keV (due mainly to Fe) have larger cross-sections than the shielded resonances. The contribution from inelastic cross-section to the total cross-section is appreciable. High energy neutrons at front locations are mainly slowed down by inelastic collisions. The inelastically scattered neutrons by these resonances tend to have energies in the range of 10-100 keV. Higher (unshielded) cross-section at these resonances simply means larger number of scattered neutrons in the 10-100 keV range. This increase peaks somewhere around 0.1-0.15 m depth. Likewise, the gamma rays emitted from these inelastic reactions will also increase with the unshielded cross-sections and that increase could be felt at deeper locations (up to a depth 0f 0.45 m, see the discussion on gamma ray heating below) due to their transport in media.

5. Lower Energy Ranges: The C/E values of the integrated spectrum in the energy ranges 1-10 keV, 0.1-1 keV, 10-100 eV and 1-10 eV have the following features in Assembly #2 where low energy neutrons were measured by BF3 counters.

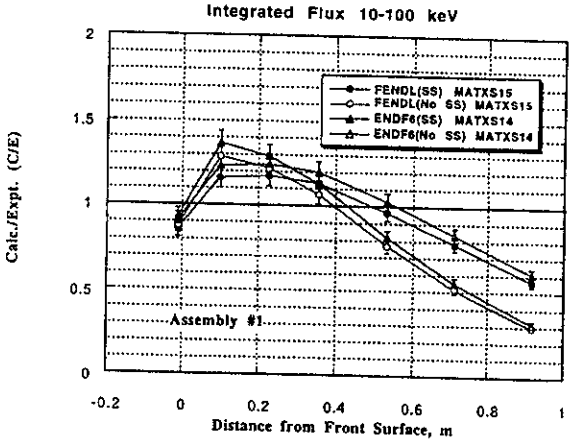

Figure 14: The C/E Values of the Integrated Neutron Flux in the Energy Range 10-100 keV-FENDL/MG

a) Based on the FENDL/MG shielded library, the C/E of the integrated spectrum at depth 0.355 m is larger than unity by 10% in the first two energy ranges (0.1-10 keV, see Fig. 18) and by ~30% in the energy range 1-100 eV (see Fig. 19). The experimental errors assigned to the integrated spectrum below 10 keV is ~ 10%. Therefore, the calculated integrated spectrum in the first two energy ranges is within the experimental errors. The over prediction of ~30% in the energy range 1-100 eV at front locations can also be seen from the MC results shown in Fig. 20. With the FENDL/MG data, the over prediction starts to lessen till under prediction is observed beyond 0.45 m (energy range 0.1-10 keV) and beyond 0.65 m (energy range 1-100 eV). The under prediction is ~ 35-40% in the energy ranges 0.1-10 keV and 1-100 eV at depth 0.914m. The

corresponding under prediction obtained with the unshielded data is ~ 65%. These under prediction at deep locations is not observed with the FENDL/MC data, as can be seen from Fig. 20 where the calculated values are within the experimental errors (~10%).

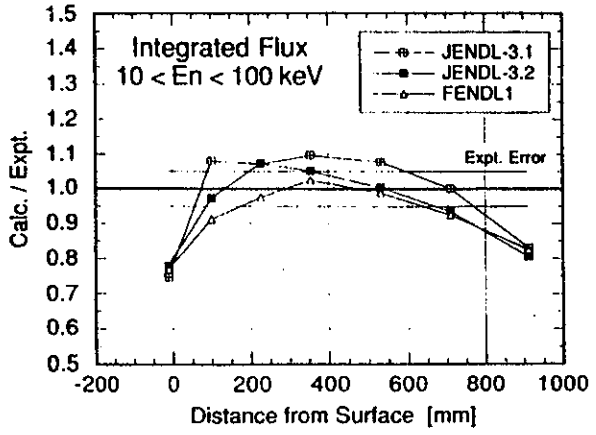

Figure 15: The C/E Values of the Integrated Neutron Flux in the Energy Range 10-100 keV-FENDL/MC

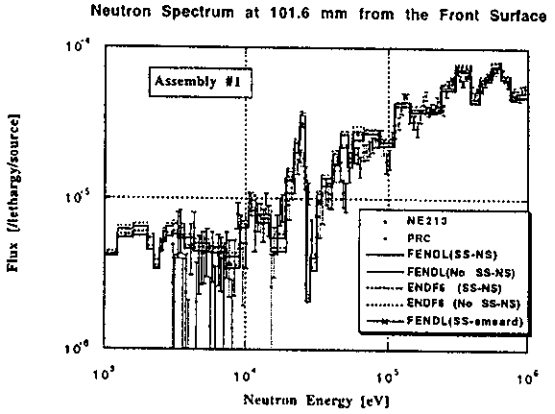

Figure 16: Measured and Calculated Neutron Spectra in the keV energy Region at Depth 101.6 mm in Assembly #1

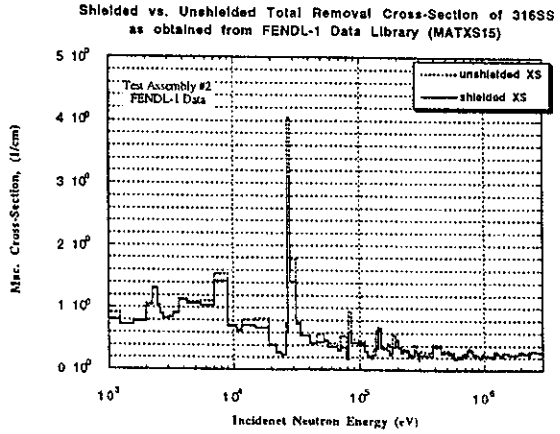

Figure 17: Shielded VS.. Unshielded Total Removal Cross-Section of SS316 as Obtained from FENDL/MG-1 Data Library (MATXS15) - [En 10^3-10^8 eV]

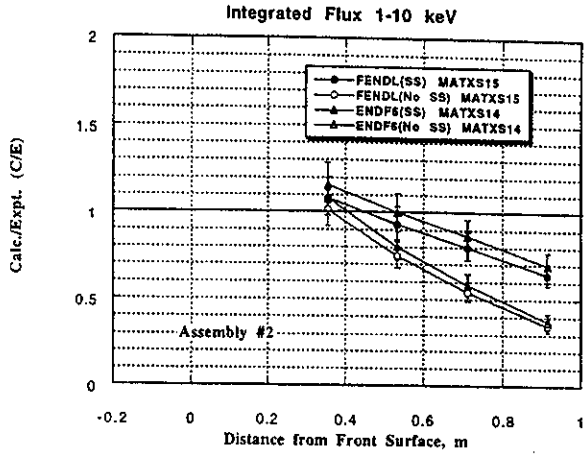

Figure 18: The C/E Values of the Integrated Neutron Flux in the Energy Range 1-10 keV-FENDL/MG

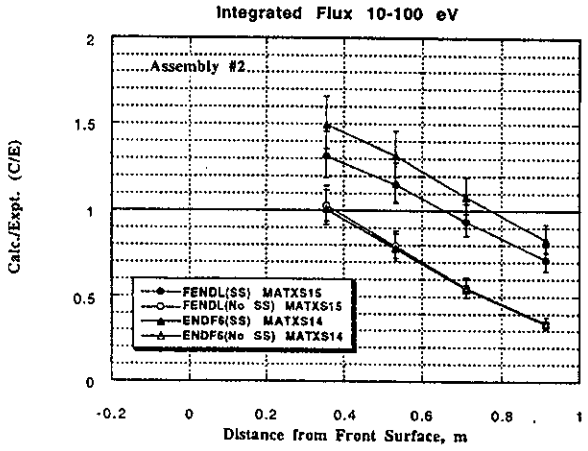

Figure 19: The C/E Values of the Integrated Neutron Flux in the Energy Range 10-100 eV- FENDL/MG

(b) The integrated spectrum obtained by ENDF6/MG shielded data is ~ 5-10% larger than the one obtained with FENDL/MG shielded library in the energy range 0.1-10 keV. This difference becomes larger by 20-25% at lower energies (1-100 eV).

(c) FENDL/MG and ENDF6/MG unshielded data give similar integrated spectra in the four energy ranges.

Note: The features of the C/E curves obtained with the FENDL/MG and MC data for the integrated spectrum in

the energy rage 1-10 eV are almost identical to the corresponding curves in the energy range 10-100 eV.

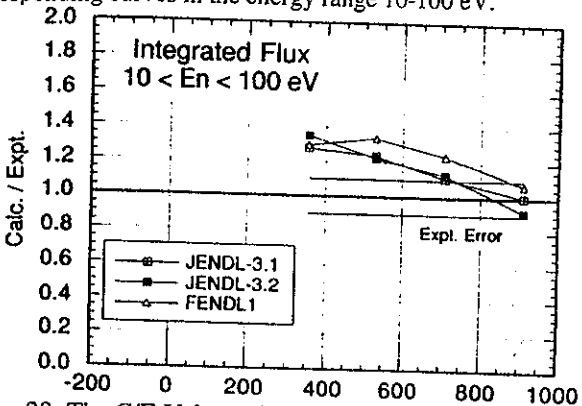

Figure 20: The C/E Values of the Integrated Neutron Flux in the Energy Range 10-100 eV- FENDL/MC

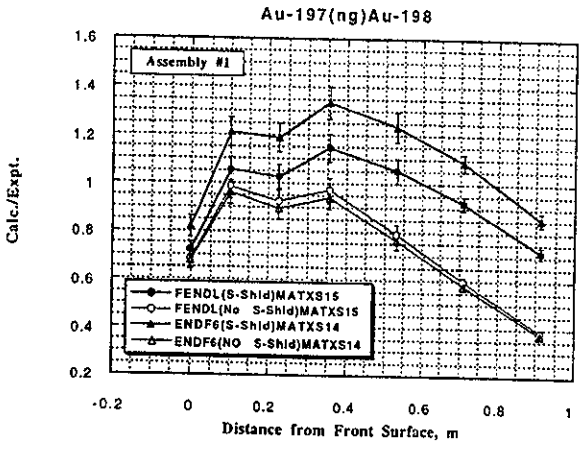

Figure 21: The C/E values for $^{197}Au(n,g)^{198}Au$ - FENDL/MG (Assembly #1)

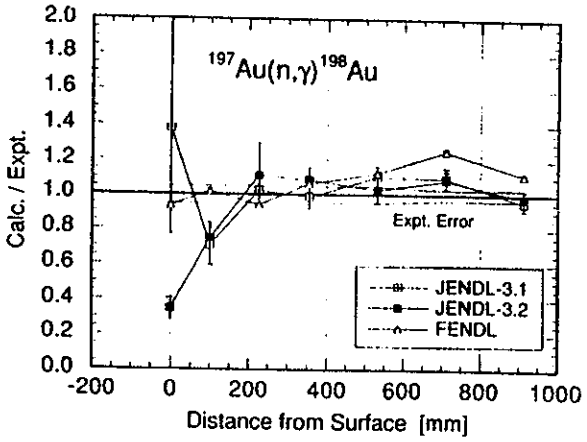

Figure 22: The C/E values for $^{197}Au(n,g)^{198}Au$ - FENDL/MC (Assembly #1)

The impact of the above features on $^{197}Au(n,g)^{198}Au$ reaction rate can be seen in Figs 21 and 22. Except for the first measuring location at 0.0 m, the C/E of the reaction rate obtained by FENDL/MG shielded data is larger than unity by ~ 15% at a depth of 0.355 m and the over prediction decreases by depth. Consistent with the under prediction in the integrated spectrum of low energy neutrons discussed above for the MG data, the under prediction in this reaction rate at depth 0.914 m is ~ 30% in both assemblies with the shielded FENDL/MG data. The corresponding under prediction with the unshielded data is 65%. The shielded ENDF6/MG data gives larger calculated values than the corresponding FENDL/MG data by ~20%. Severe under prediction (60-65%) is also obtained with the unshielded ENDF6/MG data at depth 0.914m, the value of which is consistent with the underprediction mentioned in (a) above.

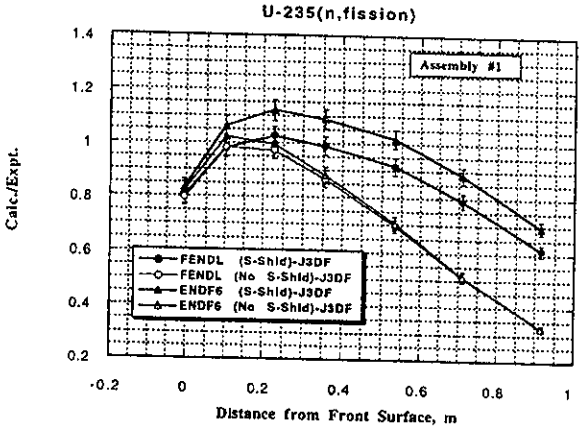

Figure 23: The C/E values for $^{235}U(n,f)$- FENDL/MG-

The results based on FENDL/MC data show different trend. as can be seen from Fig. 22. The $^{197}Au(n,g)^{198}Au$ reaction is well predicted with tendency to overestimation for locations deep inside the steel block. This is also true for the $^{235}U(n,f)$ reaction rate, i.e. the FENDL/MG shielded data tends to overestimate the reaction by ~15% at front locations and underestimation of ~ 40% occurs at depth 0.914 m (see Fig. 23). Unshielded data amounts to ~65% under prediction at this deep location and the unshielded FENDL/MG and ENDF6/MG data give similar results but not the shielded ones. On the other hand, results based on FENDL/MC data have different features where the C/E values are below unity by 5-15% at almost all locations as shown in Fig. 24.

B. Gamma rays Nuclear Heating

The total heating in the SS316 block is dominated by gamma ray heating, particularly at deep locations. It was shown that neglecting the self-shielding correction in FENDL/MG calculations leads to factors of ~ 1.8, 2.4, and

1.8 reduction in the calculated total heating, neutron heating, and gamma ray heating in both assemblies at

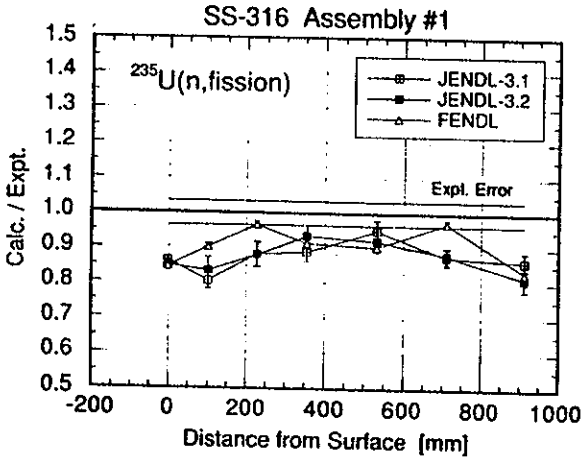

Figure 24: The C/E values for ^{235}U(n,f)- FENDL/MC

depth 1.1176m. At lesser depth (0.914 m), the reduction factors are about 1.6, 1.9, 1.6 in both assemblies and with both data bases.

The C/E values of gamma ray heating rates are shown in Figs. 25 for Ass.#1. Based on FENDL/MG shielded data, values are lower than unity at front location , above unity (by ~10% maximum) for a depth of 0.45 m, then the values steadily fall below unity thereafter. The under prediction at depth 0.914 m is ~40% (70% with the unshielded data). The C/E curves for the shielded and unshielded cross-section cases of FENDL/MG cross each other at depth 0.45 m (Assembly #1) and at 0.35 (Assembly #2). At shallower locations smaller than these depths, the unshielded data gives larger calculated gamma ray heating rate than the shielded data. Gamma heating at these front locations are dominated by the gammas emitted from high-energy inelastic reactions whereas the gamma heating at the deep locations are dominated by gammas emitted from capture reactions (n,g). As mentioned earlier, the rather larger gamma heating rates with the unshielded data could be due to the enhanced number of gamma rays emitted from the unshielded inelastic resonances in the 10-100 keV range whose cross-sections are higher than the shielded ones. The Monte Carlo results show that gamma ray heating is under predicted at almost all locations. The underestimation is stronger a the front positions (by ~20%) and at deep locations inside the block (by ~30%). The calculated values however lie within the experimental errors at front locations as shown in Fig. 26.

C. Comparison between FENDL/MG-1 and ENDF/B-VI/MG Results:

It was shown that the results based on ENDF6/MG shielded data are larger than those based on FENDL/MG shielded data by ~5-20% for high-threshold reaction rates and integrated spectrum down to neutron energy of 0.1 keV. The difference becomes more (20-25%) at lower energies (1-100 eV). This is also true for reaction rate that are sensitive to low-energy neutrons [e.g. ^{97}Au(n,g)^{198}Au and ^{235}U(n,f)] and for gamma ray heating. It is to be noted that the cross sections of the main constituents of SS316 (Fe, Cr, Ni) in FENDL/MG are derived from the ENDF/B-VI evaluations while differences in the cross-sections of constituents derived from other evaluations (e.g. Mo, Si) should not impact the results since their atomic densities are one order of magnitude less than that of iron.

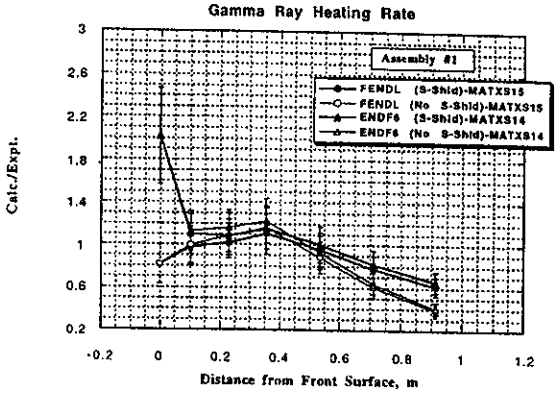

Figure 25: The C/E Values of Gamma Ray Heating in Assembly #1-FENDL/MG

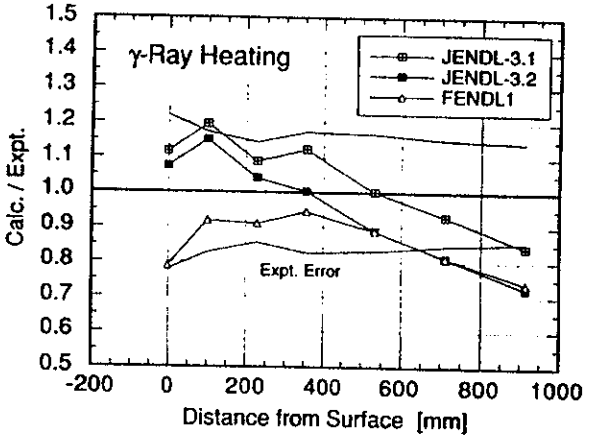

Figure 26: The C/E Values of Gamma Ray Heating in Assembly #1-FENDL/MC

Figure 27 show a comparison of the 175n multigroup shielded total neutron cross-section of SS316 derived from FENDL/MG (MATXS15) and ENDF6/MG (MATXS14) in 175n group structure. The cross-sections are almost identical below ~ 3 MeV but large differences could be seen above this energy. The σt of ENDF6/MG is larger than the σt of FENDL/MG by ~3%, ~15%, and ~18% at energies 4, 14, and 16 MeV, respectively. One would expect that by having larger total cross-section, the integrated spectra above 2 MeV would be lower in the ENDF6 case at deep locations compared to results based on FENDL data. This

is not the case. This discrepancy requires further investigation. It is possible that the procedures followed in processing the ENDF6 point base data (particularly energy and angular distribution data) were different in the course of generating the MATXS15 and MATXS14 multigroup libraries.

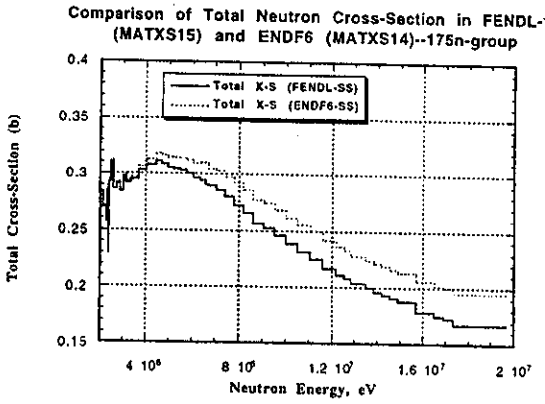

Figure 27: Comparison of Total Neutron Cross-Section in FENDL/MG-1 (MATXS15) and ENDF/B-VI/MG (MATXS14) 175n Group ($2x10^6$-$2x10^7$ eV)

D. Comparison Between Results Based on FENDL/MG and FENDL/MC for Low-Energy Reactions

While the features of the C/E curves based on FENDL/MG and MC data are similar for high-threshold reactions and the integrated spectrum above 0.1 keV, they differ for non-threshold reaction, gamma ray heating, and integrated spectrum below 0.1 keV. In multigroup libraries, the effective absorption (and fission) cross-sections are weighted with a maxwalian distribution for thermal neutrons. This could result in larger effective values than the case when the actual harder spectrum (as in pure SS316 media) is used as the weighting function. The larger (n,g) cross-section for the thermal group in the FENDL/MG data could explain the rather larger $^{97}Au(n,g)^{198}Au$ reaction rates at front locations shown in Fig. 21 (excluding the first measuring point) compared to the results based on the FENDL/MC data (Fig. 22). Like wise, large (n, fission) cross-section leads to the large C/E values for $^{235}U(n,f)$ at shallow locations (Fig. 23) compared to FENDL/MC results (Fig. 24). Larger absorption (and fission) rates at front locations leads to lower integrated spectrum for low-energy neutrons. This can be seen in Figs. 19 and 20 where the C/E values are lower in the FENDL/MG case than the values obtained with the FENDL/MC data up to a depth of ~ 0.6 m. One therefore should be cautious with this inherent limitation in the discrete ordinates calculations unless the low-energy and thermal groups are properly evaluated.

V. CONCLUDING SUMMARY

FENDL/MG-1.0 (multigroup, MG) and FENDL/MC (Monte Carlo, MC) data bases have been developed recently for use in ITER/EDA phase and are benchmarked in the present work by making comparison to experimental data from two SS316 bulk shield experiments. The objectives of the benchmarking are: (a) to identify deficiencies, if any, in FENDL/-1.0 data and (b) to verify the adequacy of the libraries in predicting neutronics parameters at deep locations inside a thick shield and quantify ranges of uncertainties (design margins) of calculated parameters that impact magnet protection scheme in ITER· As a reference, the analysis was also performed with ENDF/B-VI multigroup data for cross-checking. Results based on shielded and unshielded multigroup data were compared.

Accuracies in predicting neutron spectrum were examined directly by comparing calculations to measured spectrum and indirectly by making comparison to various reaction rates measured by foil activation technique. Comparison to measured data on gamma ray heating were also made. The following can be stated:

A. No major flaws clearly stand out in FENDL/MG-1.0 and FENDL/MC-1.0, at least for the elements constituting SS316 (Fe, Cr, Ni, Mo, etc) that cause large deviations from the predictions obtained by the reference ENDF/B-VI data. The features of the calculated parameters are similar with the two data bases, however, the systematic larger values obtained by the ENDF/B-VI/MG data requires further investigation.

B. Large discrepancies were found between measurements and calculations at deep locations inside the assemblies. The prediction accuracies found are:

(1) underestimation of the high energy neutron flux (E>10 MeV) of 25-35% at deep locations when using MG data and to about 10% when using MC data. Reactions that are sensitive to this neutron component are also underestimated at these locations by as much as ~20%. Self-shielding the cross-section has no impact on the calculated values of these high-energy reactions,

(2) for neutron spectrum in the energy range 2 to 10 MeV, a strong overestimation is observed in the integrated spectrum at the front locations, which turns into an underestimation of ~ 10%, both with MG and MC calculations at deep locations.

(3) in the MC calculations, the deviations from the measured values are in general smaller and there is a tendency to agree with the measurements within the experimental error,

(4) In the energy range 0.1 to 1 MeV, there is again an underestimation observed in the neutron spectra that amounts up to 40 % with the MG data whereas MC results show ~ 15% underestimation,

(5) below 0.1 MeV there is an underestimation in the integrated spectrum at deep locations and an over estimation (in the MG results) at the front part. The MC calculations tend to agree with the measurements within the experimental error. The $^{197}Au(n,g)$ reaction rate (sensitive to this energy range) is well predicted by MC calculations with a tendency to overestimation for the locations deep inside the steel block. In the MG calculations, however, there is a different trend: overestimations in the middle part of the block and strong underestimations at the back positions. These features are similar in the MG calculations for the $^{235}U(n,f)$ reactions and for gamma-ray heating. This could be due to the rather larger effective absorption (and fission) cross-section of the thermal group caused by using maxwellian distribution as the weighting function rather than using a harder spectrum (as in pure SS316) instead. Self-shielded data gives better agreement with measurements for non-threshold reactions and for gamma ray heating at deep locations.

In summary, there is a trend (in both the MG and MC calculations) of underestimating the integrated spectrum in the energy ranges En>10 MeV and 2<En<10 MeV at deep locations. The under estimation is severe (up to 60% in some cases) with the MG data (MATXS15). The MG data is sensitive to the processing procedures followed to generate these data. It was shown recently by Konno[20] that by using σ_0 of 1 for ^{56}Fe rather than the values of $10,100,1000,10^4,10^5$ for all the isotopes of iron, and applying the self-shielding correction, better agreement with measurements were obtained and the large under estimation observed here was lessened. It can be stated, however, that the MC calculations agree better with measurements particularly for low energy reactions. The observed discrepancies in these integral experiments could be used as bases for qualitatively estimating design safety factors for ITER shield design. For example, from the under estimation of ~25-35% in the integrated spectrum above 10 MeV with the MG data (~10% for 2 MeV<En< 10 MeV) one can apply a conservative safety factor of ~1.4 when calculating damage parameters to the RF coil which is mainly caused by fast (high-energy) neutrons reaching the SC magnet. Likewise, the under prediction of ~40% in low-energy component of the neutron flux calculated with the MG data could be compensated for by applying a safety factor of ~1.4 to calculated parameters that are sensitive to low-energy neutrons such as heating rate in the SC magnet. This heating rate is dominated by gamma-ray heating . These gamma-rays are mainly originated from the capture of low-energy neutrons at these deep locations.

ACKNOWLEDGMENT

This work is supported by the U.S. Department of Energy grant#DOE-FG03-88ER52150. The experimental data has been provided by JAERI as a part of joint collaboration with the US according to the agreement reached in Garching March 21-26, 1994.

REFERENCES

1. GANESAN, S., and MUIR, D.W.,"FENDL Multigroup Libraries," IAEA-NDS-129, International Atomic Energy Agency, July 1992.

2. "ITER Conceptual Design Report," ITER Documentation Series, No 18, IAEA, Vienna, 1991.

3. GLASS, A.J. ,"Status and Plans for ITER," J. of Fusion Energy, Vol. 11, No. 2, 1992.

4. DAENNER W., et al.,"Neutron Shielding and its Impact on the ITER Machine Design," Fusion Engr. & Design, 16, 183-193, 1991.

5. GANESAN, S., "Improved Evaluations and Integral Data Testing for FENDL: Summary Report of the IAEA Advisory Group Meeting organized by the International Atomic Energy Agency in co-operation with MAX-Planck Institut fur Plasmaphysik, Garching near Munich, Germany, 12-16 December, 1994, INDC(NDS)-312, International Nuclear Data Committee, IAEA, November, 1994.

6. "The IAEA Advisory Group Meeting on Completion of FENDL-1 and Start of FENDL-2", December 5-9, 1995, Del Mar, California, 1995.

7. EL-GUEBALY, L.A.,"Magnet Shielding Effectiveness of the Proposed Blankets for ITER," Proc. of the 14th IEEE/NPSS Symposium on Fusion Engineering, Sep. 30-Oct. 3, 1991, San Diego, USA, 1991.

8. EL-GUEBALY, L.A., and SAWAN, M.E.,"Shielding Considerations for ITER: Current Status and Future Directions," Proc. Conf. of New Horizon in Radiation Protection and Shielding, April 26- May 1, 1992, Pasco, Washington, 1992.

9. M.Z. YOUSSEF, et al., "Benchmarking FENDL-1.0 Library Through Analysis Of Existing Experiments, Part (I): Analysis Of Bulk Shielding Experiments On Large SS316 Assemblies Bombarded By D-T Neutrons", ITER/US/95/IV-BL-14A, UCLA-FNT-90, UCLA-ENG-94-40, University of California, Los Angeles, Dec., 1996.

10.)C. KONNO, F. MAEKAWA, Y. OYAMA, Y. IKEDA, K. KOSAKO, and H. MAEKAWA, "Bulk Shielding Experiments on Large SS316 Assemblies Bombarded By D-T Neutrons, Volume I: Experiment", JAERI-Research-94-043, Japan Atomic Energy Research Institute, December, 1994.

11. F. MAEKAWA, C. KONNO, K. KOSAKO, Y. OYAMA, Y. IKEDA, and H. MAEKAWA, "Bulk

Shielding Experiments on Large SS316 Assemblies Bombarded By D-T Neutrons, Volume II: Analysis", JAERI-Research-94-044, Japan Atomic Energy Research Institute, December, 1994.

12. KONNO, C., et al., "Pre-Analyses of SS316 and SS316/Water Bulk Shielding Experiments," JAERI-Tech 94-19, 1994.

13. R.E. MACFARLANE, "TRANSX2: A Code for Interfacing MATXS Cross-Section, Libraries to Nuclear Transport Codes," LA-12312-MS, UC-705 and UC-700 Issued: July 1992, Los Alamos National Laboratory, 1992.

14. R.E. MACFARLANE, Los Alamos National Laboratory, private communication, 1994.

15. NAKAZAWA, M., et al., "JENDL Dosimetry File," JAERI- 1325, 1992.

16. "ANISN-ORNL: One Dimensional Discrete Ordinates Transport Code System with Anisotropic Scattering", CCC-254, Radiation Shielding Information Center, RSIC.

17. M. NAKAGAWA and T. MORI, "MORSE--DD, A Monte Carol Code Using Multigroup Double Differential Form Cross-Sections" JAERI-M84-126, Japan Atomic Energy Research Institute, July, 1984.

18. L.P. KU and J. KOLIBAL. "RUFF-A Ray Tracing Program to Generate Uncollided Flux and First Collision Source Moments for DOT4. A User's Manual. EAD-R-16, Plasma Physics Laboratory, Princeton University, 1980.

19. RHOADES, W.A., and CHILDS, R.L.,"The DORT: Two-Dimensional Discrete Ordinates Transport Code", Nuc. Sci.&Engrg., 99, pp. 88-89 (May 1988), Also, see CCC-484, Radiation Shielding Information Center, 1988.

20. C. KONNO, "Problem of FENDL/MG-1.0", Task-218 Review Meeting, March 25-27, 1996, ITER Garching Joint Work Site, Garching, Germany, 1996.